Editors' Suggestion

Many-Body Quantum Interference Route to the Two-Channel Kondo Effect: Inverse Design for Molecular Junctions and Quantum Dot Devices

Sudeshna Sen[1] and Andrew K. Mitchell[2,3,*]
[1]Department of Physics, IIT(ISM) Dhanbad, Dhanbad-826004 Jharkhand, India
[2]School of Physics, University College Dublin, Belfield, Dublin 4, Ireland
[3]Centre for Quantum Engineering, Science, and Technology, University College Dublin, Dublin, Ireland

(Received 27 October 2023; revised 22 May 2024; accepted 15 July 2024; published 12 August 2024)

Molecular junctions—whether actual single molecules in nanowire break junctions or artificial molecules realized in coupled quantum dot devices—offer unique functionality due to their orbital complexity, strong electron interactions, gate control, and many-body effects from hybridization with the external electronic circuit. Inverse design involves finding candidate structures that perform a desired function optimally. Here we develop an inverse design strategy for generalized quantum impurity models describing molecular junctions, and as an example, use it to demonstrate that many-body quantum interference can be leveraged to realize the two-channel Kondo critical point in simple 4- or 5-site molecular moieties. We show that remarkably high Kondo temperatures can be achieved, meaning that entropy and transport signatures should be experimentally accessible.

DOI: 10.1103/PhysRevLett.133.076501

Nanoelectronics circuits are quantum devices featuring a nanostructure with a few confined and typically strongly correlated degrees of freedom coupled to source and drain metallic leads [1–5]. For molecular junctions, a single molecule can bridge the gap in a nanowire [6]. The electrical conductance of such a junction is controlled by the structure and chemistry of the molecule, through which a current must pass [7]. A range of physics can be realized in such systems—including Coulomb blockade [8] and various Kondo effects [4,9–15], quantum interference [16–23], and phase transitions [24,25]. This presents the tantalizing possibility of devices at the limit of miniaturization that leverage inherently quantum effects to provide enhanced functionality as switches [26–29], transistors [4,5], diodes and rectifiers [30–35], and even as tools for chemical analysis [36]. A grand challenge is to find molecular species that can form robust junctions to perform a desired function optimally [37].

Simple artificial molecular junctions can also be fabricated in semiconductor coupled quantum dot (QD) devices [38,39]. The design of such systems need not obey chemical structure principles [40], and they benefit from *in-situ* tunability [41,42]. They can also be integrated with other components to realize more exotic effects, such as fractionalization at the two-channel Kondo (2CK) quantum critical point [43], which results from the frustration of screening when a single spin-$\frac{1}{2}$ degree of freedom is coupled to two independent conduction electron channels [44]. The 2CK effect has gained prominence recently as a route to engineer many-body Majorana zero modes in nanostructures [45–48]. Spectacular experimental realizations of 2CK physics in QD systems [49–51] have however required the use of a 'quantum box' or metallic island to provide a reservoir of many interacting electrons [52,53]. Can the 2CK effect be realized in simpler QD systems without the use of these components? If so, what is the minimum number of interacting sites needed? Can we find molecular moieties that realize 2CK physics when placed in a junction?

Model—Molecular junctions and QDs are described by generalized quantum impurity models [54] of the form $\hat{H} = \hat{H}_{\rm mol} + \hat{H}_{\rm leads} + \hat{H}_{\rm hyb} + \hat{H}_{\rm gate}$. Here we formulate the isolated molecule as an extended Hubbard Hamiltonian,

$$\hat{H}_{\rm mol} = \sum_{\sigma=\uparrow,\downarrow}\sum_{m,n} t_{mn} d^\dagger_{m\sigma} d_{n\sigma} + \frac{1}{2}\sum_{m,n} U_{mn}\hat{n}_m\hat{n}_n \qquad (1)$$

where $d^{(\dagger)}_{m\sigma}$ annihilates (creates) an electron on molecule orbital m with spin σ and $\hat{n}_m = \sum_\sigma d^\dagger_{m\sigma} d_{m\sigma}$ is a number operator. Single-particle processes are parameterized by t_{mn} whereas U_{mn} embodies electronic interactions. The gate voltage V_g controls the charge on the molecule via $\hat{H}_{\rm gate} = V_g \sum_m \hat{n}_m$. The leads are described by continua of free fermions, $\hat{H}_{\rm leads} = \sum_{\alpha,\sigma} \epsilon_k c^\dagger_{\alpha\sigma k} c_{\alpha\sigma k}$ with $\alpha = s,\ d$ for source and drain. The molecule frontier orbital $d_{r_\alpha\sigma}$ couples to a local orbital $c_{\alpha\sigma}$ of lead α via $\hat{H}_{\rm hyb} = \sum_{\alpha,\sigma} V_\alpha (d^\dagger_{r_\alpha\sigma} c_{\alpha\sigma} + {\rm H.c.})$, where $c_{\alpha\sigma} = (1/V_\alpha)\sum_k V_k c_{\alpha\sigma k}$.

Strong electron interactions [3,4] produce rich many-body physics but also preclude brute force solutions [54].

*Contact author: Andrew.Mitchell@UCD.ie

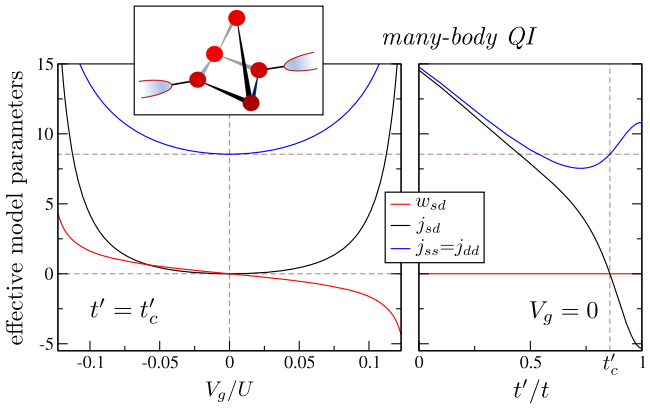

FIG. 1. The simplest molecular moiety to exhibit the 2CK effect with 5 interacting active orbitals. The effective molecule-lead Kondo interactions j_{ss} and j_{dd} are equal and antiferromagnetic (blue line), while source-drain mixing terms vanish due to many-body QI. Potential scattering w_{sd} (red) vanishes at gate voltage $V_g = 0$ by particle-hole symmetry, whereas exchange cotunneling j_{sd} (black) vanishes on tuning the couplings t'/t. Obtained here via SWT and plotted for $U/t = 1$.

Inverse design is challenging because physical properties then depend in a highly nontrivial way on the delicate interplay of many microscopic parameters. It is a formidable task to find a set of model parameters that yield specific device functionalities. However, if only the *low-temperature* behavior is of interest, then simpler low-energy effective models may be used [55–57]. The connection between effective model parameters and low-temperature physical properties is typically far more transparent.

Here we focus on one such scenario, where the low-temperature physics that we seek is that of the 2CK critical point [58]. The condition for obtaining this behavior in molecular junctions is simply stated in terms of the low-energy effective 2CK model. Inverse design then consists of finding the set of microscopic model parameters satisfying this condition. We show that this is achievable in remarkably simple systems, with just a few interacting degrees of freedom, and without the interacting electron reservoirs used previously in experiments [49–51].

Effective models—An odd number of electrons can be accommodated on the molecule by tuning gate voltages, such that the ground state of $\hat{H}_{\rm mol}$ is a unique spin-doublet state. At low temperatures, effective spin-flip Kondo exchange interactions and potential scattering are generated, described by a generalized 2CK model [59],

$$\hat{H}_{\rm eff} = \hat{H}_{\rm leads} + \sum_{\alpha,\beta}\left[J_{\alpha\beta}\hat{\vec{\mathbb{S}}}\cdot\hat{\vec{s}}_{\alpha\beta} + W_{\alpha\beta}\sum_{\sigma} c^{\dagger}_{\beta\sigma}c_{\alpha\sigma}\right] \quad (2)$$

where $\hat{\vec{\mathbb{S}}}$ is a spin-$\frac{1}{2}$ operator for the molecule ground state doublet and $\hat{\vec{s}}_{\alpha\beta} = \frac{1}{2}\sum_{ss'} c^{\dagger}_{\beta s'}\vec{\boldsymbol{\sigma}}_{s's}c_{\alpha s}$ are conduction electron spin operators. We refer to the $J_{\alpha\beta}$ and $W_{\alpha\beta}$ terms as exchange and potential scattering, respectively. The form of Eq. (2) is guaranteed by $SU(2)$ spin symmetry if only the most RG relevant terms are considered [21]. Since $J_{sd} = J_{ds}$ and $W_{sd} = W_{ds}$ by hermiticity, the low-energy behavior of such molecular junctions is controlled by just six effective parameters.

The 2CK critical point arises for equal antiferromagnetic Kondo interactions $J_{ss} = J_{dd} > 0$, but when the source-drain mixing terms vanish, $J_{sd} = W_{sd} = 0$ [58,75]. In molecular junctions or coupled QD devices, the 2CK effect should be realizable when the molecule or QD has a net spin-$\frac{1}{2}$ ground state and when the effective model parameters satisfy these conditions. W_{ss} and W_{dd} are RG irrelevant and play no role in the following.

Quantum interference (QI) and conductance nodes—Single-molecule junctions often exhibit QI phenomena, with the most dramatic effect being electrical conductance nodes due to the destructive interference of competing transport pathways through the molecule [17–20]. However, such a description of the QI and transport is typically on the single-particle level encoded by the real-space hopping matrix t_{nm} [76], and is inapplicable for interacting systems displaying Coulomb blockade or Kondo effects. Although sequential single-particle tunneling processes may be afflicted by decoherence at weak coupling [8], coherent many-body processes are more robust at low temperatures in interacting systems [77]. Many-body QI [21,78] is naturally richer than its single-particle counterpart, being defined in a high-dimensional Fock space, and provides new channels for QI (e.g. between particles and holes). Many-body QI can cause any of the parameters $J_{\alpha\beta}$ and $W_{\alpha\beta}$ to vanish in the effective 2CK model Eq. (2). $J_{sd} = W_{sd} = 0$ must produce a conductance node because then the charge in the leads is separately conserved. The 2CK critical point therefore arises at a conductance node, which can be driven by many-body QI. We dub this the QI-2CK effect.

Perturbative solution—We consider first the perturbative derivation of the effective 2CK parameters from those of the bare model by means of a generalized Schrieffer-Wolff transformation (SWT) [55]. This is done by projecting the full model for the junction onto the spin-doublet molecule ground states by eliminating virtual excitations to second order in $\hat{H}_{\rm hyb}$. In the Supplemental Material [59] we formulate this problem in an efficient way that does not require full diagonalization of $\hat{H}_{\rm mol}$, but only uses information on the ground state energy and wavefunction of the isolated molecule. Comparatively large systems can then be treated by using methods that target ground state properties [79–81].

Eq. (2) is obtained by SWT with effective parameters $J_{\alpha\beta} \equiv V_\alpha V_\beta j_{\alpha\beta}$ and $W_{\alpha\beta} \equiv V_\alpha V_\beta w_{\alpha\beta}$ that can be calculated from many-body scattering amplitudes $A^{\sigma\alpha\beta} = p^{\sigma\alpha\beta} - h^{\sigma\alpha\beta}$ which involve the tunneling of both particles (p) and holes (h) with spin-σ through the molecule from lead α to lead β. We

may write $j_{\alpha\beta}=2(A^{\uparrow\alpha\beta}-A^{\downarrow\alpha\beta})$ and $w_{\alpha\beta}=\frac{1}{2}(A^{\uparrow\alpha\beta}+A^{\downarrow\alpha\beta})$, with the p and h amplitudes obtainable in closed form as detailed in the Supplemental Material [59].

Many body QI can appear here in different ways: through the vanishing of individual p or h processes due to interference of competing Fock space propagators, by a cancellation of terms with different spin, or by a cancellation of p and h amplitudes for a given process.

In fact, particle-hole (ph) symmetry guarantees the latter, since then $p^{\sigma\alpha\beta}=h^{-\sigma\alpha\beta}$ and hence $W_{ss}=W_{dd}=W_{sd}=0$ in Eq. (2). A system is ph-symmetric when its Hamiltonian is invariant to the ph transformations $d_{n\sigma}\to e^{i\phi_{n\sigma}}d^{\dagger}_{n\sigma}$ for all $n\sigma$ (with suitable phases $\phi_{n\sigma}$). The celebrated Coulson-Rushbrooke pairing theorem [82] is a statement about ph symmetry, with p and h excitations appearing symmetrically around the ground state for molecules satisfying the 'starring rule' [78,83]. A system may exhibit ph symmetry if the molecular structure encoded by the single-particle adjacency matrix t_{mn} can be accommodated on a bipartite graph. Therefore ph-symmetric systems must *not* have odd loops.

Satisfying the 2CK condition—Since ph symmetry implies $W_{sd}=0$, we search for ph-symmetric systems in which $J_{sd}=0$ can also be achieved. In addition we want $J_{ss}=J_{dd}$ for the 2CK effect so we consider only sd-symmetric molecular moieties. As a simple starting point we study M-site Hubbard chains with constant nearest neighbour hopping t, local Coulomb repulsion U, and local potential $\epsilon=-U/2$. Leads s and d are connected to molecule sites 1 and M. For odd M the ground state around $V_g=0$ is a unique spin-doublet and we numerically perform the SWT as shown in the Supplemental Material [59]. The system is ph-symmetric at $V_g=0$ such that $W_{\alpha\beta}=0$. We also find $J_{ss}=J_{dd}>0$. Although J_{sd} is always finite, we find that its sign alternates for $M=1,3,5,7,\ldots$. In particular, $J_{sd}<0$ for $M=3$ but $J_{sd}>0$ for $M=5$. One might anticipate that interpolating between $M=3$ and $M=5$ might yield a sweet spot solution where $J_{sd}=0$. Avoiding odd loops and preserving sd symmetry, this can be achieved by connecting sites 1 to 4 and 2 to 5, viz:

$$H_{\rm mol}=\frac{U}{2}\sum_{m=1}^{5}(\hat{n}_m-1)^2+t\sum_{\sigma}\sum_{m=1}^{4}\left(d^{\dagger}_{m\sigma}d_{m+1\sigma}+\text{H.c.}\right)+t'\sum_{\sigma}\left(d^{\dagger}_{1\sigma}d_{4\sigma}+d^{\dagger}_{2\sigma}d_{5\sigma}+\text{H.c.}\right). \quad (3)$$

For small t'/t we expect small perturbations to the $M=5$ chain solution, whereas for large t'/t the next-next-nearest-neighbour tunneling provides a shortcut through the chain so that only 3 sites are needed to connect s and d leads. Numerical results of the SWT are presented in Fig. 1, together with a schematic illustration of the junction. At ph symmetry $V_g=0$, the effective model parameters are plotted as a function of t'/t in the right panel. We indeed confirm that $j_{sd}=0$ at a special value $t'=t'_c$ (black line). In the left panel we show the gate evolution of the same parameters at $t'=t'_c$, with the 2CK conditions being satisfied here at $V_g=0$.

Non-perturbative solution: NRG—To confirm the existence of a 2CK critical point in this simple 5-site molecular cluster, we turn to the non-perturbative solution of the full molecular junction involving Eq. (3) using NRG [84], where we set $t=\frac{1}{2}$ and the conduction electron bandwidth $D=1$ from now on. Numerical results are presented in Fig. 2. In panel (a) we compare SWT predictions for the critical t'_c with those obtained by NRG for different interaction strengths U, showing excellent agreement. In particular, we note that the 2CK critical point can be realized for *any* finite U. Interestingly, we find that $t'_c\to t$ as $U\to 0$. The $U=0$ limit of Eq. (3) is studied in the Supplemental Material [59]: we find $t'=t$ is a singular point of the non-interacting model with strictly decoupled molecular degrees of freedom that give a finite $T=0$ entropy and a QI-driven conductance node. With interactions switched on, the critical t'_c is no longer at t but we still find a residual $T=0$ entropy and a conductance node—now characterizing the 2CK critical fixed point. Panel (c) shows the molecular contribution to the entropy $S_{\rm mol}$ as a function of T at the critical point for different V. The critical point can be realized for any combination of V and U (in panel (c) we take fixed U), and in all cases we find $S_{\rm mol}=\frac{1}{2}\ln(2)$ for $T\ll T_{\rm K}$, with $T_{\rm K}$ the critical Kondo

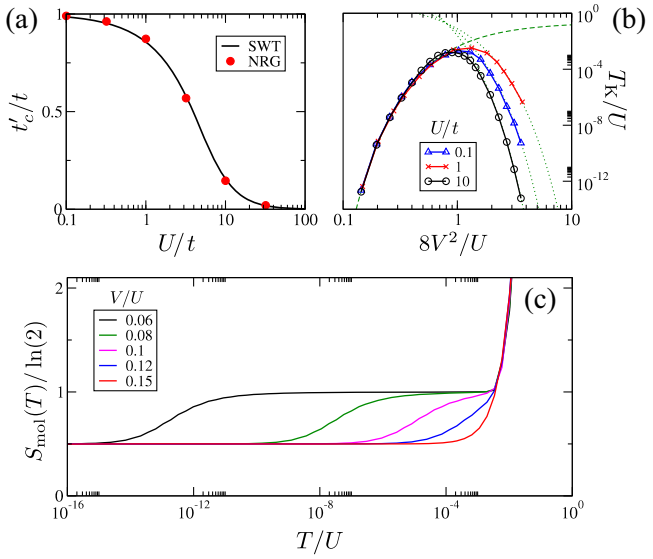

FIG. 2. 2CK critical point driven by QI. (a) Critical coupling t'_c as a function of U/t, with NRG results (points) validating SWT predictions (line). (b) 2CK Kondo temperature $T_{\rm K}$ vs $8V^2/U\equiv J_K$ for different U/t obtained by NRG. Dashed line is $T_{\rm K}/U\sim\exp[-4/J_K]$ valid for $J_K<1$ whereas the dotted lines show $T_{\rm K}/U\sim\exp[-aJ_K]$ with $a\equiv a(U)\sim\mathcal{O}(1)$ for $J_K>1$. (c) Entropy $S_{\rm mol}$ vs T/U for different V/U at the 2CK critical point for $U/t=10$, showing a residual $\frac{1}{2}\ln(2)$.

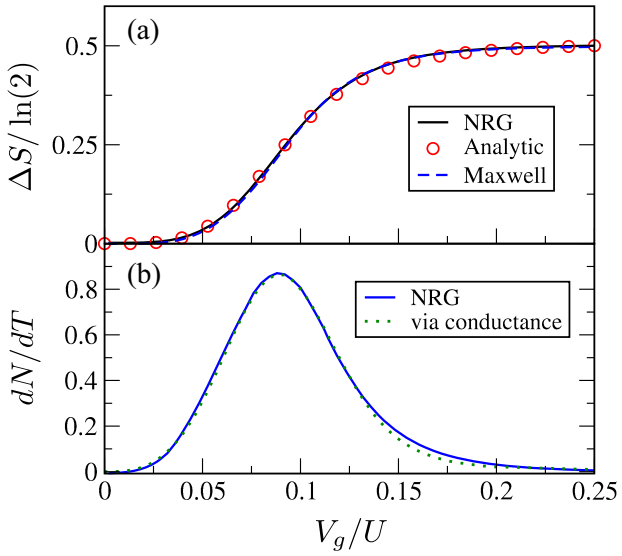

FIG. 3. (a) Entropy change ΔS as the molecular junction is driven away from the critical point by increasing gate voltage V_g. NRG results (line) compared with analytic result Eq. (5) (points). (b) dN/dT from NRG (line), compared with prediction via conductance from Eq. (7) (dotted line). Dashed line in the top panel obtained by integrating dN/dT over V_g. Plotted for $U/t = 10$, $V/U = 0.15$, $t' = t'_c$, $T = 10^{-6} \ll T_K$.

temperature. This unusual value for the entropy is a hallmark of the free Majorana fermion localized on the molecule at low temperatures at the 2CK critical point [45,58]. For small molecule-lead coupling, T_K is small and we have an extended intermediate ln(2) plateau corresponding to the local moment regime of Eq. (2). Remarkably however, at larger V the Kondo temperature can be boosted to large (non-universal) values and local moment physics is entirely eliminated. This scenario lies outside of the regime described by Eq. (2), suggesting that the interference giving rise to criticality is a topological feature of the geometry in Eq. (3). In Fig. 2(b) we plot the evolution of the Kondo temperature with $8V^2/U \equiv J_K$ (where J_K is the SWT Kondo coupling for a single Anderson impurity [54]), showing that a maximum value $T_K \sim 10^{-2}U$ can be realized for all values of U considered when $J_K \sim 1$. A weak-strong coupling duality [85] is found on further increasing J_K—see dashed and dotted lines in Fig. 2(b). Note that the critical point is a non-Fermi liquid and as such is not perturbatively connected to the $U = 0$ limit: even though the critical point can be realized at small U, we find that $T_K \to 0$ as $U \to 0$.

Gate control and entropy measurement—With t' tuned to the 2CK critical point at t'_c, we can vary the gate voltage V_g in the vicinity of $V_g = 0$. This perturbation drives the system away from the 2CK fixed point and towards a standard Kondo strong-coupling Fermi liquid (FL) state on the scale of T^*. From NRG we find [59],

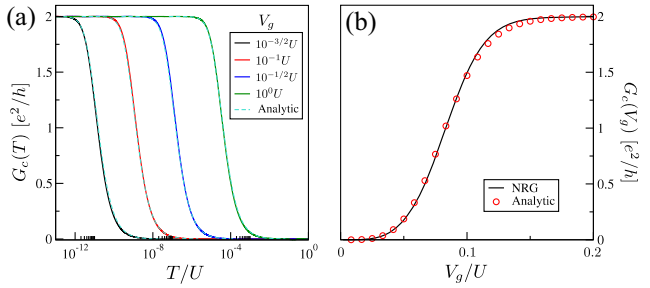

FIG. 4. Series conductance along the FL crossover (a) as a function of temperature for different gate voltages; and (b) as a function of gate voltage at fixed $T = 10^{-6} \ll T_K$; compared with Eq. (6). Shown for $U/t = 10$, $V/U = 0.15$, $t' = t'_c$.

$$T^* \sim V_g^4 \text{ when } T^* \ll T_K, \tag{4}$$

which holds in the universal critical regime. Along this FL crossover, physical properties are universal scaling functions of T^*/T and hence $V_g/T^{1/4}$. For the pure 2CK model in this regime, bosonization methods give an exact result for the entropy change from the critical point [45],

$$\Delta S\left(\frac{T^*}{T}\right) = \frac{T^*}{T}\left[\psi\left(\frac{1}{2}+\frac{T^*}{T}\right) - 1\right] - \ln\left[\frac{1}{\sqrt{\pi}}\Gamma\left(\frac{1}{2}+\frac{T^*}{T}\right)\right] \tag{5}$$

with Γ (ψ) the gamma (digamma) function. The form of this crossover is entirely characteristic of the 2CK critical point [75]. Using Eq. (4), this crossover can be achieved by fixing T ($\ll T_K$) and detuning V_g (which controls T^*). This is shown in the top panel of Fig. 3, which compares NRG results for the junction (line) to Eq. (5) (points).

Recent progress has been made in observing entropic signatures in nanoelectronics experiments, by exploiting local Maxwell relations which connect the entropy change for a process to measureable changes in the charge [86–88]. Since the gate voltage V_g couples to the total molecule charge $\hat{N} = \sum_m \hat{n}_m$, the change in entropy induced by scanning V_g as in Fig. 3(a) follows as $\Delta S = -\int dV_g dN/dT$. The quantity dN/dT is shown in Fig. 3(b). Application of the Maxwell relation yields the blue-dashed line in Fig. 3(a), which agrees perfectly with the direct entropy calculation. We argue that the molecular system is well suited to this because T_K can be boosted to large values, meaning that the universal critical regime should be experimentally accessible.

Transport—At the 2CK critical point, the series conductance through the molecular junction vanishes due to the many-body QI node. However, a nontrivial transport signature is picked up along the FL crossover by detuning the gate voltage. NRG results for the junction conductance $G_c(T)$ as a function of T at fixed detuning V_g are shown in Fig. 4(a). The maximum conductance of $2e^2/h$ for a single electron transistor is recovered at low temperatures $T \ll T^*$ in all cases. Figure 4(b) shows the gate evolution of the

conductance $G_c(V_g)$ at fixed T ($\ll T_K$), and is the analogous plot to Fig. 3(a).

The exact solution of the pure 2CK model along the FL crossover [45] yields a prediction for conductance [89],

$$G_c\left(\frac{T^*}{T}\right) = \frac{2e^2}{h} \times \left(\frac{T^*}{T}\right)\psi'\left(\frac{1}{2}+\frac{T^*}{T}\right), \tag{6}$$

where T^* depends on V_g via Eq. (4) and ψ' is the trigamma function. This expression matches essentially perfectly with NRG data for the full molecular junction in Fig. 4.

Finally, from the Maxwell relation $dN/dT = -dS/dV_g$ we can use Eqs. (4)–(6) to prove the exact conductance-charge relation [87] in the universal FL crossover regime,

$$\frac{dN}{dT} \sim \frac{V_g^3}{T}\left(1 - \frac{G_c(V_g,T)}{2e^2/h}\right), \tag{7}$$

meaning that experimental conductance data can be translated into dN/dT [see Fig. 3(b), dotted line] and then integrated to extract the entropy.

Inverse design—The above results establish the existence of the QI-2CK effect in a simple molecular moiety with exact *ph* and *sd* symmetry. In a more general setting, however, we can use inverse design to search for candidate systems that satisfy the 2CK conditions. This can be done by setting up a loss function, for example $\mathcal{L} = j_{sd}^2 + w_{sd}^2 + (j_{ss} - j_{dd})^2$, which is minimum when the 2CK conditions on the effective model parameters are met. We then minimize this function with respect to the bare model parameters by gradient descent (GD). In practice this involves finding the derivatives of $j_{\alpha\beta}$ and $w_{\alpha\beta}$ with respect to t_{mn} and U_{mn}, which can be achieved using differentiable programming techniques [90]. In the Supplemental Material [59] we show that this can be implemented very efficiently within our improved SWT scheme. Using this methodology, we could find a family of low-symmetry molecular junctions involving just 4 interacting sites [59], a representative example of which is shown in Fig. 5. By fine-tuning the gate voltage V_g in this structure we predict 2CK criticality. We did not find any 2CK critical systems involving 1, 2, or 3 sites.

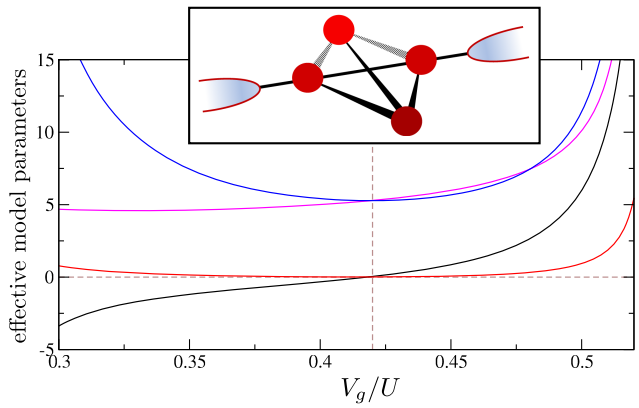

FIG. 5. Inverse design of a four-site molecular junction using GD optimization of effective SWT parameters to realize the QI-2CK condition at gate voltage $V_g/U = 0.42$. Black: j_{sd}; red: w_{sd}; magenta: j_{ss}; blue: j_{dd}. Parameters given in [59].

A nonperturbative extension utilizing 'differentiable NRG' [91] to optimize bare model parameters directly via GD could be used to bypass the SWT approximation.

Conclusion—The 2CK critical point can be realized by exploiting many-body QI effects in simple molecular junctions or coupled quantum dot devices, featuring a few tunnel-coupled, interacting orbitals. QI effects can be manipulated by tuning gate voltages to switch between a perfect node and perfect Kondo resonant transmission.

Inverse design can be used to search automatically for systems displaying desired functionality. The molecular moieties we identified are not intended to be atomistic models of any real molecule. However, the inverse design approach could be integrated with chemical databases to search for realistic candidate molecular junctions [92]. In the Supplemental Material [59] we explore three such candidate molecules based on the simple design principles uncovered from our toy model studies [59]. Full *ab initio* studies are left for future work. On the other hand, for artificial molecular junctions formed in semiconductor quantum dot devices, the simplest 4 or 5 site structures discussed here might be directly implementable.

Our results open the door to designer devices utilizing many-body QI effects. For example, simple structures exhibiting three-channel Kondo [59,93] or two-impurity Kondo [94–96] effects, or lattice extensions describing non-Fermi liquid materials [97]. Inverse design could be used to optimize performance of nanoscale transistors, rectifiers, spintronics devices, and other quantum devices.

Acknowledgments—This work was supported by the Irish Research Council through the Laureate Award 2017/2018 Grant No. IRCLA/2017/169 and by Science Foundation Ireland through Grant No. 21/RP-2TF/10019 (A. K. M.) and Science and Engineering Research Board, India (SRG/2022/000495), (MTR/2022/000638), and IIT (ISM) Dhanbad [FRS(175)/2022-2023/PHYSICS] (S .S.). We thank Jonas Rigo for enlightening discussions.

[1] L. P. Kouwenhoven, D. Austing, and S. Tarucha, Few-electron quantum dots, Rep. Prog. Phys. **64**, 701 (2001).
[2] R. Hanson, L. P. Kouwenhoven, J. R. Petta, S. Tarucha, and L. M. K. Vandersypen, Spins in few-electron quantum dots, Rev. Mod. Phys. **79**, 1217 (2007).
[3] D. Goldhaber-Gordon, H. Shtrikman, D. Mahalu, D. Abusch-Magder, U. Meirav, and M. Kastner, Kondo effect in a single-electron transistor, Nature (London) **391**, 156 (1998); S. M. Cronenwett, T. H. Oosterkamp, and L. P. Kouwenhoven, A tunable Kondo effect in quantum dots, Science **281**, 540 (1998).

[4] J. Park, A. N. Pasupathy, J. I. Goldsmith, C. Chang, Y. Yaish, J. R. Petta, M. Rinkoski, J. P. Sethna, H. D. Abruña, P. L. McEuen *et al.*, Coulomb blockade and the Kondo effect in single-atom transistors, Nature (London) **417**, 722 (2002); W. Liang, M. P. Shores, M. Bockrath, J. R. Long, and H. Park, Kondo resonance in a single-molecule transistor, Nature (London) **417**, 725 (2002).
[5] M. L. Perrin, E. Burzurí, and H. S. van der Zant, Single-molecule transistors, Chem. Soc. Rev. **44**, 902 (2015).
[6] A. R. Champagne, A. N. Pasupathy, and D. C. Ralph, Mechanically adjustable and electrically gated single-molecule transistors, Nano Lett. **5**, 305 (2005).
[7] B. Xu and N. J. Tao, Measurement of single-molecule resistance by repeated formation of molecular junctions, Science **301**, 1221 (2003).
[8] J. M. Thijssen and H. S. Van der Zant, Charge transport and single-electron effects in nanoscale systems, Phys. Status Solidi (b) **245**, 1455 (2008).
[9] J. Paaske, A. Rosch, P. Wölfle, N. Mason, C. Marcus, and J. Nygård, Non-equilibrium singlet–triplet Kondo effect in carbon nanotubes, Nat. Phys. **2**, 460 (2006).
[10] N. Roch, S. Florens, T. A. Costi, W. Wernsdorfer, and F. Balestro, Observation of the underscreened Kondo effect in a molecular transistor, Phys. Rev. Lett. **103**, 197202 (2009).
[11] J. Parks, A. Champagne, T. Costi, W. Shum, A. Pasupathy, E. Neuscamman, S. Flores-Torres, P. Cornaglia, A. Aligia, C. Balseiro *et al.*, Mechanical control of spin states in spin-1 molecules and the underscreened Kondo effect, Science **328**, 1370 (2010).
[12] X. Guo, Q. Zhu, L. Zhou, W. Yu, W. Lu, and W. Liang, Evolution and universality of two-stage Kondo effect in single manganese phthalocyanine molecule transistors, Nat. Commun. **12**, 1566 (2021).
[13] P. Zalom, J. De Bruijckere, R. Gaudenzi, H. S. Van Der Zant, T. Novotny, and R. Korytár, Magnetically tuned Kondo effect in a molecular double quantum dot: Role of the anisotropic exchange, J. Phys. Chem. C **123**, 11917 (2019).
[14] P. Lucignano, R. Mazzarello, A. Smogunov, M. Fabrizio, and E. Tosatti, Kondo conductance in an atomic nanocontact from first principles, Nat. Mater. **8**, 563 (2009).
[15] R. Requist, S. Modesti, P. P. Baruselli, A. Smogunov, M. Fabrizio, and E. Tosatti, Kondo conductance across the smallest spin $1/2$ radical molecule, Proc. Natl. Acad. Sci. U.S.A. **111**, 69 (2014).
[16] C. A. Stafford, D. M. Cardamone, and S. Mazumdar, The quantum interference effect transistor, Nanotechnology **18**, 424014 (2007).
[17] C. M. Guédon, H. Valkenier, T. Markussen, K. S. Thygesen, J. C. Hummelen, and S. J. Van Der Molen, Observation of quantum interference in molecular charge transport, Nat. Nanotechnol. **7**, 305 (2012).
[18] Y. Li, M. Buerkle, G. Li, A. Rostamian, H. Wang, Z. Wang, D. R. Bowler, T. Miyazaki, L. Xiang, Y. Asai *et al.*, Gate controlling of quantum interference and direct observation of anti-resonances in single molecule charge transport, Nat. Mater. **18**, 357 (2019).
[19] J. Bai, A. Daaoub, S. Sangtarash, X. Li, Y. Tang, Q. Zou, H. Sadeghi, S. Liu, X. Huang, Z. Tan *et al.*, Anti-resonance features of destructive quantum interference in single-molecule thiophene junctions achieved by electrochemical gating, Nat. Mater. **18**, 364 (2019).
[20] J. E. Greenwald, J. Cameron, N. J. Findlay, T. Fu, S. Gunasekaran, P. J. Skabara, and L. Venkataraman, Highly nonlinear transport across single-molecule junctions via destructive quantum interference, Nat. Nanotechnol. **16**, 313 (2021).
[21] A. K. Mitchell, K. G. Pedersen, P. Hedegård, and J. Paaske, Kondo blockade due to quantum interference in single-molecule junctions, Nat. Commun. **8**, 1 (2017).
[22] A. N. Pal, D. Li, S. Sarkar, S. Chakrabarti, A. Vilan, L. Kronik, A. Smogunov, and O. Tal, Nonmagnetic single-molecule spin-filter based on quantum interference, Nat. Commun. **10**, 5565 (2019).
[23] D. Li, R. Banerjee, S. Mondal, I. Maliyov, M. Romanova, Y. J. Dappe, and A. Smogunov, Symmetry aspects of spin filtering in molecular junctions: Hybridization and quantum interference effects, Phys. Rev. B **99**, 115403 (2019).
[24] N. Roch, S. Florens, V. Bouchiat, W. Wernsdorfer, and F. Balestro, Quantum phase transition in a single-molecule quantum dot, Nature (London) **453**, 633 (2008).
[25] S. Florens, A. Freyn, N. Roch, W. Wernsdorfer, F. Balestro, P. Roura-Bas, and A. Aligia, Universal transport signatures in two-electron molecular quantum dots: Gate-tunable Hund's rule, underscreened Kondo effect and quantum phase transitions, J. Phys. Condens. Matter **23**, 243202 (2011).
[26] E. Lörtscher, J. W. Ciszek, J. Tour, and H. Riel, Reversible and controllable switching of a single-molecule junction, Small **2**, 973 (2006).
[27] S. Y. Quek, M. Kamenetska, M. L. Steigerwald, H. J. Choi, S. G. Louie, M. S. Hybertsen, J. Neaton, and L. Venkataraman, Mechanically controlled binary conductance switching of a single-molecule junction, Nat. Nanotechnol. **4**, 230 (2009).
[28] S. J. van der Molen and P. Liljeroth, Charge transport through molecular switches, J. Phys. Condens. Matter **22**, 133001 (2010).
[29] J. L. Zhang, J. Q. Zhong, J. D. Lin, W. P. Hu, K. Wu, G. Q. Xu, A. T. Wee, and W. Chen, Towards single molecule switches, Chem. Soc. Rev. **44**, 2998 (2015).
[30] M. Elbing, R. Ochs, M. Koentopp, M. Fischer, C. von Hänisch, F. Weigend, F. Evers, H. B. Weber, and M. Mayor, A single-molecule diode, Proc. Natl. Acad. Sci. U.S.A. **102**, 8815 (2005).
[31] M. L. Perrin, E. Galán, R. Eelkema, J. M. Thijssen, F. Grozema, and H. S. van der Zant, A gate-tunable single-molecule diode, Nanoscale **8**, 8919 (2016).
[32] A. Batra, P. Darancet, Q. Chen, J. S. Meisner, J. R. Widawsky, J. B. Neaton, C. Nuckolls, and L. Venkataraman, Tuning rectification in single-molecular diodes, Nano Lett. **13**, 6233 (2013).
[33] I. Díez-Pérez, J. Hihath, Y. Lee, L. Yu, L. Adamska, M. A. Kozhushner, I. I. Oleynik, and N. Tao, Rectification and stability of a single molecular diode with controlled orientation, Nat. Chem. **1**, 635 (2009).
[34] R. M. Metzger, Unimolecular electrical rectifiers, Chem. Rev. **103**, 3803 (2003).
[35] R. Gupta, J. A. Fereiro, A. Bayat, A. Pritam, M. Zharnikov, and P. C. Mondal, Nanoscale molecular rectifiers, Nat. Rev. Chem. **7**, 106 (2023).

[36] E. M. Dief, P. J. Low, I. Díez-Pérez, and N. Darwish, Advances in single-molecule junctions as tools for chemical and biochemical analysis, Nat. Chem. **15**, 600 (2023).
[37] N. Xin, J. Guan, C. Zhou, X. Chen, C. Gu, Y. Li, M. A. Ratner, A. Nitzan, J. F. Stoddart, and X. Guo, Concepts in the design and engineering of single-molecule electronic devices, Nat. Rev. Phys. **1**, 211 (2019).
[38] L. Kouwenhoven, Coupled quantum dots as artificial molecules, Science **268**, 1440 (1995).
[39] H. Jeong, A. M. Chang, and M. R. Melloch, The Kondo effect in an artificial quantum dot molecule, Science **293**, 2221 (2001).
[40] R. P. Feynman, There's plenty of room at the bottom, *Feynman and Computation* (CRC Press, 2018), pp. 63–76.
[41] P. Barthelemy and L. M. Vandersypen, Quantum dot systems: A versatile platform for quantum simulations, Ann. Phys. (Berlin) **525**, 808 (2013).
[42] N. Petropoulos, X. Wu, A. Sokolov, P. Giounanlis, I. Bashir, A. Mitchell, M. Asker, D. Leipold, R. B. Staszewski, and E. Blokhina, Nanoscale single-electron box with a floating lead for quantum sensing: Modeling and device characterization, Appl. Phys. Lett. **124** (2024).
[43] I. Affleck and A. W. W. Ludwig, Universal noninteger "ground-state degeneracy" in critical quantum systems, Phys. Rev. Lett. **67**, 161 (1991).
[44] P. Nozieres and A. Blandin, Kondo effect in real metals, J. Phys. **41**, 193 (1980).
[45] V. J. Emery and S. Kivelson, Mapping of the two-channel Kondo problem to a resonant-level model, Phys. Rev. B **46**, 10812 (1992).
[46] Y. Komijani, Isolating Kondo anyons for topological quantum computation, Phys. Rev. B **101**, 235131 (2020).
[47] M. Lotem, E. Sela, and M. Goldstein, Manipulating non-Abelian anyons in a chiral multichannel Kondo model, Phys. Rev. Lett. **129**, 227703 (2022).
[48] P. L. S. Lopes, I. Affleck, and E. Sela, Anyons in multichannel Kondo systems, Phys. Rev. B **101**, 085141 (2020).
[49] R. Potok, I. Rau, H. Shtrikman, Y. Oreg, and D. Goldhaber-Gordon, Observation of the two-channel Kondo effect, Nature (London) **446**, 167 (2007).
[50] A. Keller, L. Peeters, C. Moca, I. Weymann, D. Mahalu, V. Umansky, G. Zaránd, and D. Goldhaber-Gordon, Universal Fermi liquid crossover and quantum criticality in a mesoscopic system, Nature (London) **526**, 237 (2015).
[51] Z. Iftikhar, S. Jezouin, A. Anthore, U. Gennser, F. Parmentier, A. Cavanna, and F. Pierre, Two-channel Kondo effect and renormalization flow with macroscopic quantum charge states, Nature (London) **526**, 233 (2015).
[52] Y. Oreg and D. Goldhaber-Gordon, Two-channel Kondo effect in a modified single electron transistor, Phys. Rev. Lett. **90**, 136602 (2003).
[53] A. Furusaki and K. A. Matveev, Theory of strong inelastic cotunneling, Phys. Rev. B **52**, 16676 (1995).
[54] A. Hewson, *The Kondo Problem to Heavy Fermions* (Cambridge University Press, Cambridge, England, 1993).
[55] J. R. Schrieffer and P. A. Wolff, Relation between the anderson and Kondo Hamiltonians, Phys. Rev. **149**, 491 (1966); S. Bravyi, D. P. DiVincenzo, and D. Loss, Schrieffer–Wolff transformation for quantum many-body systems, Ann. Phys. (Amsterdam) **326**, 2793 (2011).
[56] J. B. Rigo and A. K. Mitchell, Machine learning effective models for quantum systems, Phys. Rev. B **101**, 241105(R) (2020).
[57] J. B. Rigo and A. K. Mitchell, Unsupervised model learning for quantum impurity systems, arXiv:2401.13600.
[58] I. Affleck and A. W. Ludwig, Exact conformal-field-theory results on the multichannel Kondo effect: Single-fermion Green's function, self-energy, and resistivity, Phys. Rev. B **48**, 7297 (1993).
[59] See Supplemental Material at http://link.aps.org/supplemental/10.1103/PhysRevLett.133.076501 for further details of (i) the models; (ii) our new SWT formalism; (iii) analysis of many-body QI classes; (iv) NRG calculations; (v) the 2CK critical point and (vi) its FL crossover; (vii) the role of vibrations; (viii) ML optimization; (ix) the noninteracting $U = 0$ limit; (x) candidate molecular junctions to realize QI-2CK; and (xi) an outlook towards the QI-3CK effect. The Supplemental Material contains additional Refs. [60–74].
[60] L. Lafferentz, F. Ample, H. Yu, S. Hecht, C. Joachim, and L. Grill, Conductance of a single conjugated polymer as a continuous function of its length, Science **323**, 1193 (2009).
[61] R. Chan and M. Gulácsi, The exact Schrieffer–Wolff transformation, Philos. Mag. **84**, 1265 (2004).
[62] F. Haldane, Theory of the atomic limit of the Anderson model. I. Perturbation expansions re-examined, J. Phys. C **11**, 5015 (1978).
[63] A. K. Mitchell, D. E. Logan, and H. R. Krishnamurthy, Two-channel Kondo physics in odd impurity chains, Phys. Rev. B **84**, 035119 (2011).
[64] E. L. Minarelli, J. B. Rigo, and A. K. Mitchell, Linear response quantum transport through interacting multi-orbital nanostructures, arXiv:2209.01208.
[65] R. Kubo, Statistical-mechanical theory of irreversible processes. I. General theory and simple applications to magnetic and conduction problems, J. Phys. Soc. Jpn. **12**, 570 (1957).
[66] L. H. Yu, Z. K. Keane, J. W. Ciszek, L. Cheng, M. P. Stewart, J. M. Tour, and D. Natelson, Inelastic electron tunneling via molecular vibrations in single-molecule transistors, Phys. Rev. Lett. **93**, 266802 (2004).
[67] S. Ballmann, R. Härtle, P. B. Coto, M. Elbing, M. Mayor, M. R. Bryce, M. Thoss, and H. B. Weber, Experimental evidence for quantum interference and vibrationally induced decoherence in single-molecule junctions, Phys. Rev. Lett. **109**, 056801 (2012).
[68] A. Hewson and D. Meyer, Numerical renormalization group study of the Anderson-Holstein impurity model, J. Phys. Condens. Matter **14**, 427 (2001).
[69] J. Paaske and K. Flensberg, Vibrational sidebands and the Kondo effect in molecular transistors, Phys. Rev. Lett. **94**, 176801 (2005).
[70] L. G. G. V. Dias da Silva and E. Dagotto, Phonon-assisted tunneling and two-channel Kondo physics in molecular junctions, Phys. Rev. B **79**, 155302 (2009).
[71] D. P. Clougherty, Endohedral impurities in carbon nanotubes, Phys. Rev. Lett. **90**, 035507 (2003).
[72] P. Lucignano, G. E. Santoro, M. Fabrizio, and E. Tosatti, Two-level physics in a model metallic break junction, Phys. Rev. B **78**, 155418 (2008).

[73] R. P. Feynman, Forces in molecules, Phys. Rev. **56**, 340 (1939).
[74] R. Landauer, Spatial variation of currents and fields due to localized scatterers in metallic conduction, IBM J. Res. Dev. **1**, 223 (1957).
[75] E. Sela, A. K. Mitchell, and L. Fritz, Exact crossover Green function in the two-channel and two-impurity Kondo models, Phys. Rev. Lett. **106**, 147202 (2011); A. K. Mitchell and E. Sela, Universal low-temperature crossover in two-channel Kondo models, Phys. Rev. B **85**, 235127 (2012).
[76] C. Lambert, Basic concepts of quantum interference and electron transport in single-molecule electronics, Chem. Soc. Rev. **44**, 875 (2015).
[77] J. König and Y. Gefen, Coherence and partial coherence in interacting electron systems, Phys. Rev. Lett. **86**, 3855 (2001).
[78] K. G. L. Pedersen, M. Strange, M. Leijnse, P. Hedegård, G. C. Solomon, and J. Paaske, Quantum interference in off-resonant transport through single molecules, Phys. Rev. B **90**, 125413 (2014).
[79] E. R. Gagliano, E. Dagotto, A. Moreo, and F. C. Alcaraz, Correlation functions of the antiferromagnetic Heisenberg model using a modified Lanczos method, Phys. Rev. B **34**, 1677 (1986).
[80] U. Schollwöck, The density-matrix renormalization group in the age of matrix product states, Ann. Phys. (Amsterdam) **326**, 96 (2011).
[81] D. Zgid, E. Gull, and G. K.-L. Chan, Truncated configuration interaction expansions as solvers for correlated quantum impurity models and dynamical mean-field theory, Phys. Rev. B **86**, 165128 (2012).
[82] C. Coulson and G. Rushbrooke, Note on the method of molecular orbitals, in *Mathematical Proceedings of the Cambridge Philosophical Society* (Cambridge University Press, Cambridge, England, 1940), Vol. 36, pp. 193–200.
[83] Y. Tsuji, E. Estrada, R. Movassagh, and R. Hoffmann, Quantum interference, graphs, walks, and polynomials, Chem. Rev. **118**, 4887 (2018).
[84] K. G. Wilson, The renormalization group: Critical phenomena and the Kondo problem, Rev. Mod. Phys. **47**, 773 (1975); R. Bulla, T. A. Costi, and T. Pruschke, Numerical renormalization group method for quantum impurity systems, Rev. Mod. Phys. **80**, 395 (2008).
[85] C. Kolf and J. Kroha, Strong versus weak coupling duality and coupling dependence of the Kondo temperature in the two-channel Kondo model, Phys. Rev. B **75**, 045129 (2007).
[86] N. Hartman, C. Olsen, S. Lüscher, M. Samani, S. Fallahi, G. C. Gardner, M. Manfra, and J. Folk, Direct entropy measurement in a mesoscopic quantum system, Nat. Phys. **14**, 1083 (2018).
[87] C. Han, Z. Iftikhar, Y. Kleeorin, A. Anthore, F. Pierre, Y. Meir, A. K. Mitchell, and E. Sela, Fractional entropy of multichannel Kondo systems from conductance-charge relations, Phys. Rev. Lett. **128**, 146803 (2022).
[88] T. Child, O. Sheekey, S. Lüscher, S. Fallahi, G. C. Gardner, M. Manfra, A. Mitchell, E. Sela, Y. Kleeorin, Y. Meir *et al.*, Entropy measurement of a strongly coupled quantum dot, Phys. Rev. Lett. **129**, 227702 (2022).
[89] A. K. Mitchell, L. A. Landau, L. Fritz, and E. Sela, Universality and scaling in a charge two-channel Kondo device, Phys. Rev. Lett. **116**, 157202 (2016).
[90] M. Bartholomew-Biggs, S. Brown, B. Christianson, and L. Dixon, Automatic differentiation of algorithms, J. Comput. Appl. Math. **124**, 171 (2000).
[91] J. B. Rigo and A. K. Mitchell, Automatic differentiable numerical renormalization group, Phys. Rev. Res. **4**, 013227 (2022).
[92] S. Raghunathan and U. D. Priyakumar, Molecular representations for machine learning applications in chemistry, Int. J. Quantum Chem. **122**, e26870 (2022).
[93] Z. Iftikhar, A. Anthore, A. Mitchell, F. Parmentier, U. Gennser, A. Ouerghi, A. Cavanna, C. Mora, P. Simon, and F. Pierre, Tunable quantum criticality and super-ballistic transport in a "charge" Kondo circuit, Science **360**, 1315 (2018).
[94] B. A. Jones, C. M. Varma, and J. W. Wilkins, Low-temperature properties of the two-impurity Kondo Hamiltonian, Phys. Rev. Lett. **61**, 125 (1988).
[95] A. K. Mitchell, E. Sela, and D. E. Logan, Two-channel Kondo physics in two-impurity Kondo models, Phys. Rev. Lett. **108**, 086405 (2012).
[96] W. Pouse, L. Peeters, C. L. Hsueh, U. Gennser, A. Cavanna, M. A. Kastner, A. K. Mitchell, and D. Goldhaber-Gordon, Quantum simulation of an exotic quantum critical point in a two-site charge Kondo circuit, Nat. Phys. **19**, 492 (2023).
[97] D. Cox and M. Jarrell, The two-channel Kondo route to non-Fermi-liquid metals, J. Phys. Condens. Matter **8**, 9825 (1996).